JOC*Article*

Theoretical Study on Electronic Structure and Optical Properties of Phenothiazine-Containing Conjugated Oligomers and Polymers

Li Yang,[†] Ji-Kang Feng,*[,†,‡] and Ai-Min Ren[†]

State Key Laboratory of Theoretical and Computational Chemistry, Institute of Theoretical Chemistry, Jilin University, Changchun 130023, China, and College of Chemistry, Jilin University, Changchun 130023, China

jikangf@yahoo.com

Received April 5, 2005

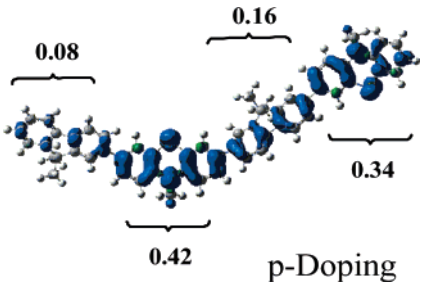

The application of polyfluorenes in polymeric light-emitting diodes has been hampered because of the charge injection difficulties and the troublesome formation of a tailed emission band at long wavelengths (>500 nm) during device fabrication and operation, leading to both a color instability and reduced efficiency. The incorporation of the phenothiazine units has been proven to significantly enhance the hole injection and charge carrier balance and at the same time efficiently suppress the keto defect emission. In this contribution, we apply quantum-chemical techniques to investigate poly[10-(*N*-(2′-methyl)phenothiazine-3,7-diyl) and its fluorene copolymer poly[10-(*N*-(2′-methyl)-phenothiazine-3,7-diyl)-*co*-*alt*-2,7-(9,9-dimethylfluorene)] (PFPTZ) and gain a detailed understanding the influence of phenothiazine units on the electronic and optical properties of fluorene derivatives. Density functional theory (DFT) and time-dependent DFT approaches are employed to study the neutral molecules, HOMO−LUMO gaps (Δ_{H-L}), the lowest excitation energies (E_g's), positive and negative ions, as well as the IPs and EAs, focusing on the superiority of the electronic and optical properties attributed to the introduction of electron-donating moiety phenothiazine (PTZ) through comparing with pristine polyfluorene. The outcomes show that the highly nonplanar conformation of phenothiazine ring in the ground state preclude sufficiently close intermolecular interactions essential to forming aggregates or excimers. Furthermore, the HOMO energies lift about 0.4 eV, and thus, the IPs decrease about 0.3 eV in PFPTZ, suggesting the significant improved hole-accepting and transporting abilities, due to the electron-donating properties of phenothiazine ring by the presence of electron-rich sulfur and nitrogen heteroatoms and highly nonplanar characters, resulting in the enhanced performances in both efficiency and brightness compared with pristine polyfluorene. In addition, even though the introduction of electron-donating moiety PTZ onto fluorene leads to a slight bathochromic shift in absorption and emission spectra, the copolymer still exhibited strong blue emission.

1. Introduction

Much effort has been undertaken recently to develop flexible and tunable light-emitting diodes from conjugated polymers.[1−7] Conducting polymers have several advantages over inorganic compounds; these are outstanding coloration efficiency, fast switching ability,[8,9] multiple colors with the same material,[10−12] and fine-tuning of the band gap (and the color) through chemical

[†] Institute of Theoretical Chemistry.
[‡] College of Chemistry.

(1) (a) Kraft, A.; Grimsdale, A. C.; Holmes, A. B. *Angew. Chem., Int. Ed. Engl.* **1998**, *37*, 402. (b) Friend, R. H.; Gymer, R. W.; Holmes, A. B.; Burroughes, J. H.; Marks, R. N.; Taliani, C.; Bradley, D. D. C.; Dos Santos, D. A.; Bre'das, J. L.; Lögdlund, M.; Salaneck, W. R. *Nature (London)* **1999**, *397*, 121. (c) Rees, I. D.; Robinson, K. L.; Holmes, A. B.; Towns, C. R.; O'Dell, R. *MRS Bull.* **2002**, *27*, 451.

10.1021/jo050665p CCC: $30.25
Published on Web 06/24/2005

structure modification.[13,14] Polyfluorene derivatives present an interesting alternative to blue-light-emitting materials as well-known highly fluorescent compounds because of their high photoluminescence (PL) quantum efficiency, thermal stability, and also their facile color tunability.[15−17] In addition to excellent luminescent properties, OLEDs also need adequate and balanced transport of both injected electrons and holes to allow an efficient recombination of these electrical charges in the luminescent chromophore. However, due to the wide energy gaps, blue luminescent polymers usually have high oxidation potentials and low electron affinities. Because of these features, polymeric blue-light-emitting devices usually face charge injection difficulties for both types of charge carriers with the currently available anode and cathode materials. Thus, many ways have been used to modulate the ionization potential (IP), electron affinity (EA), and band gaps of these polymers including conjugation length control, as well as the introduction of electron-donating or -withdrawing groups to the parent chromophore.[18−23]

Another serious problem associated with the blue-light-emitting polyfluorenes is the poor optical stability in the solid state due to $\pi-\pi$ stacking, which results in the formation of excimers or aggregates that shift emission spectra at longer wavelengths and decrease fluorescence quantum yields.[24] Recent results indicated that keto defects in the polymer backbone, originating probably from photo- and/or electrooxidative degradation of 9,9-dialkylated polyfluorenes (PFs), were mainly responsible for this strong low energy emission.[25]

In this paper, phenothiazine (PTZ),[26−30] a well-known heterocyclic compound with electron-rich sulfur and nitrogen heteroatoms, serves for a novel electron-donating unit. Its polymer poly[10-(*N*-(2′-methyl)phenothiazine-3,7-diyl) (PPTZ) and the copolymer with fluorene (PFPTZ) have been investigated in experiments,[29,30] which indicate a way to design the copolymers with enhanced hole injection and negligible low-energy emission band by modifying the chemical structures. It has been proven that the PTZ is more active than fluorene, and both PPTZ and PFPTZ exhibit very good thermal stabilities, losing less than 3% of their weight on heating to about 350 °C.[30] Here, we further explore the ground and low-lying excited states of polymers PPTZ and PFPTZ by theoretical studies, which have contributed a lot to rationalize the properties of known polymers[31−38] and to predict those of yet unknown ones.[39−41] Then we apply the experimentally well-known[36,42−48] reciprocal rule for polymers, which states that many properties of

(2) (a) Rothberg, L. J.; Lovinger, A. J. *J. Mater. Res.* **1996**, *11*, 3174. (b) Heeger, A. J. *Solid State Commun.* **1998**, *107*, 673. (c) Sheats, J. R.; Antoniadis, H.; Hueschen, M.; Leonard, W.; Miller, J.; Moon, R.; Roitman, D.; Stocking, A. *Science* **1996**, *273*, 884.
(3) (a) Tarkka, R. M.; Zhang, X.; Jenekhe, S. A. *J. Am. Chem. Soc.* **1996**, *118*, 9438. (b) Zhang, X.; Shetty, A. S.; Jenekhe, S. A. *Macromolecules* **1999**, *32*, 7422.
(4) (a) Jenekhe, S. A.; Zhang, X.; Chen, X. L.; Choong, V.-E.; Gao, Y.; Hsieh, B. R. *Chem. Mater.* **1997**, *9*, 409. (b) Zhang, X.; Jenekhe, S. A. *Macromolecules* **2000**, *33*, 2069. (c) Tonzola, C. J.; Alam, M. M.; Jenekhe, S. A. *Adv. Mater.* **2002**, *14*, 1086.
(5) (a) Gustafsson, G.; Cao, Y.; Treacy, G. M.; Klavetter, F.; Colaneri, N.; Heeger, A. J. *Nature (London)* **1992**, *357*, 477. (b) Greenham, N. C.; Moratti, S. C.; Bradley, D. D. C.; Friend, R. H.; Holmes, A. B. *Nature (London)* **1993**, *365*, 628.
(6) (a) Zhu, Y.; Alam, M. M.; Jenekhe, S. A. *Macromolecules* **2002**, *35*, 9844. (b) Zhu, Y.; Alam, M. M.; Jenekhe, S. A. *Macromolecules* **2003**, *36*, 8958.
(7) (a) Tonzola, C. J.; Alam, M. M.; Kaminsky, W.; Jenekhe, S. A. *J. Am. Chem. Soc.* **2003**, *125*, 13548. (b) Alam, M. M.; Jenekhe, S. A. *Chem. Mater.* **2002**, *14*, 4775. 5285. (b) Kulkarni, A. P.; Kong, X.; Jenekhe, S. A. *J. Phys. Chem. B.* **2004**, *108*, 8689.
(8) Sapp, S. A.; Sotzing, G. A.; Reynolds, J. R. *Chem. Mater.* **1998**, *10*, 2010.
(9) Kumar, A.; Welsh, D. M.; Morvant, M. C.; Piroux, F.; Abboud, K. A.; Reynolds, J. R. *Chem. Mater.* **1998**, *10*, 896.
(10) Brotherson, I. D.; Mudigonda, D. S. K.; Ocborn, J. M.; Belk, J.; Chen, J.; Loveday, D. C.; Boehme, J. L.; Ferraris, J. P.; Meeker, D. L. *Electrochim. Acta* **1999**, *44*, 2993.
(11) Thompson, B. C.; Schottland, P.; Zong, K.; Reynolds, J. R. *Chem. Mater.* **2000**, *12*, 1563.
(12) Thompson, B. C.; Schottland, P.; Zong, K.; Reynolds, J. R. *Synth. Met.* **2001**, *119*, 333.
(13) Sonmez, G.; Schwendeman, I.; Schottland, P.; Zong, K.; Reynolds, J. R. *Macromolecules* **2003**, *36*, 639.
(14) Schwendeman, I.; Hickman, R.; Sonmez, G.; Schottland, P.; Zong, K.; Welsh, D.; Reynolds, J. R. *Chem. Mater.* **2002**, *14*, 3118.
(15) Jenekhe, S. A.; Osaheni, J. A. *Science* **1994**, *265*, 765.
(16) Peng, Q.; Lu, Z. Y.; Huang, Y.; Xie, M. G.; Han, S. H.; Peng, J. B.; Cao, Y. *Macromolecules* **2004**, *37*, 260.
(17) Grell, M.; Bradley, D. D. C.; Inbasekaran, M.; Woo, E. P. *Adv. Mater.* **1997**, *9*, 798.
(18) Auber, P. H.; Knipper, M.; Groenendaal, L.; Lutsen, L.; Manca, J.; Vanderzande, D. *Macromolecules* **2004**, *37*, 4087.
(19) Meng, H.; Zeng, J.; Lovinger, A. L.; Wang, B. C.; Van Patter, P. G.; Bao, Z. *Chem. Mater.* **2003**, *15*, 1778.
(20) Sonmez, G.; Meng, H.; Wudl, F. *Chem. Mater.* **2004**, *16*, 574.
(21) Bouillud, A. D.; Lévesque, I.; Tao, Y.; D'Iorio, M. *Chem. Mater.* **2000**, *12*, 1931.
(22) Sonar, P.; Zhang, J.; Grimsdale, A. C.; Müllen, K. *Macromolecules* **2004**, *37*, 709.
(23) Beaupré, S.; Leclerc, M. *Adv. Funct. Mater.* **2002**, *12*, 192.
(24) (a) Bernius, M. T.; Inbasekaran, M.; O'Brien, J.; Wu, W. *Adv. Mater.* **2000**, *12*, 1737. (b) Leclerc, M. J. *Polym. Sci., Polym. Chem.* **2001**, *39*, 2867. (c) Neher, D. *Macromol. Rapid Commun.* **2001**, *22*, 1365.
(25) (a) List, E. J. W.; Guentner, R.; Freitas, P. S.; Scherf, U. *Adv. Mater.* **2002**, *14*, 374. (b) Lupton, J. M.; Craig, M. R.; Meijer, E. W. *Appl. Phys. Lett.* **2002**, *80*, 4489.
(26) Jenekhe, S. A.; Lu, L.; Alam, M. M. *Macromolecules* **2001**, *34*, 7351.
(27) Higuchi, A.; Inada, H.; Kobata, T.; Shiraota, Y. *Adv. Mater.* **1991**, *3*, 549.
(28) Lai, R. Y.; Jenekhe, S. A.; Bard, A. J. *J. Am. Chem. Soc.* **2003**, *125*, 12631.
(29) Kong, X.; Kulkarni, A. P.; Jenekhe, S. A. *Macromolecules* **2003**, *36*, 8992.
(30) Hwang, D. H.; Kim, S. K.; Park, M. J.; Lee, J. H.; Koo, B. W.; Kang, I. N.; Kim, S. H.; Zyung, T. *Chem. Mater.* **2004**, *16*, 1298.
(31) Horst, W.; Susanne, S.; Stefan, J.; Alexander, V. U.; Axel, H. E. M. *Macromolecules* **2003**, *36*, 3374−3379.
(32) Mushrush, M.; Facchetti, A.; Lefenfeld, M.; Katz, H. E.; Marks, T. J. *J. Am. Chem. Soc.* **2003**, *125*, 9414−9423.
(33) Brédas, J. L.; Silbey, R.; Boudreaux, D. S.; Chance, R. R. *J. Am. Chem. Soc.* **1983**, *105*, 6555−6559.
(34) Tavan, P.; Schulten, K. *J. Chem. Phys.* **1986**, *85*, 6602−6609.
(35) Beljonne, D.; Shuai, Z.; Cornil, J.; dos Santos, D. A.; Bredas, J. L. *J. Chem. Phys.* **1999**, *32*, 267−276.
(36) Lahti, P. M.; Obrzut, J.; Karasz, F. E. *Macromolecules* **1987**, *20*, 2023−2026.
(37) Burrows, H. D.; Seixas de Melo, J.; Serpa, C.; Arnaut, L. G.; Miguel, N. da G.; Monkman, A. P.; Hamblett, I.; Navaratnam, S. *J. Chem. Phys.* **2002**, *285*, 3−11.
(38) Scheinert, S.; Schliefke, W. *Synth. Met.* **2003**, *139*, 501−509.
(39) Yamamoto, T.; Fujiwara, Y.; Fukumoto, H.; Nakamura, Y.; Koshihara, S. Y; Ishikawa, T. *Polymer* **2003**, *44*, 4487−4490.
(40) Morisaki, Y.; Ishida, T.; Chujo, Y. *Polymer J.* **2003**, *35*, 501−506.
(41) Yang, N. C.; Chang, S.; Suh, D. H. *Polymer* **2003**, *44*, 2143−2148.
(42) Winokur, M. J.; Slinker, J.; Huber, D. L. *Phys. Rev. B* **2003**, *67*, 184106.
(43) Donat-bouillud, A.; Lévesque, L.; Tao, Y.; D'Iorio, M.; Beaupré, S.; Blondin, P.; Ranger, M.; Bouchard, J.; Leclerc, M. *Chem. Mater.* **2000**, *12*, 1931−1936.
(44) Zeng, G.; Yu, W. L.; Chua, S. J.; Huang, W. *Macromolecules* **2002**, *35*, 6907−6914.
(45) Lee, S. H.; Nakamura, T.; Tsutsui, T. *Org. Lett.* **2001**, *3*, 2005−2007.
(46) Wong, K. T.; Wang, C. F.; Chou, C. H.; Su, Y. O.; Lee, G. H.; Peng, S. M. *Org. Lett.* **2002**, *4*, 4439−4442.
(47) Ma, J.; Li, S. H.; Jiang, Y.-S. *Macromolecules* **2002**, *35*, 1109−1115.

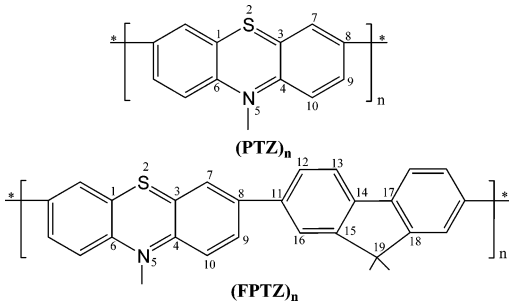

FIGURE 1. Sketch map of the structures.

homopolymers tend to vary linearly as functions of reciprocal chain lengths.[39−42] A distinct advantage of this approach is that it can provide the convergence behavior of the structural and electronic properties of oligomers. In this paper, the ground states of all the oligomers will be treated using the B3LYP functional, and the low-lying excited states will be examined using time-dependent DFT (TDDFT). The energy gap has been estimated from two ways, namely, HOMO−LUMO gaps and the lowest excited energies. We were particularly interested in exploring the highly nonplanar structural properties and the potential of phenothiazine as electron-donating moiety and the influence of different phenothiazine contents on electronic materials through comparing the energies of HOMO and LUMO and the variation of IPs, EAs, and energy gaps of PPTZ and copolymer PFPTZ with those of the PF homopolymer. The possible consequences of the nonplanarity of the phenothizaine ring for the photophysics, light-emitting properties, molecular aggregation, and charge transport of π-conjugated polymers containing this ring are very intriguing to us and thus motivated our studies. On the other hand, we wanted to show the potential of a quantum mechanical modeling based on DFT in the evaluation of ground and excited-state properties of oligomers and polymers by comparison to the available experimental data.

2. Computational Details

All calculations on these oligomers studied in this work have been performed on the SGI origin 2000 server using the Gaussian 03 program package.[49] Calculations on the electronic ground state were carried out using density functional theory (DFT), B3LYP/6-31G*. The investigated polymers $(PTZ)_n$ and $(FPTZ)_n$ (as depicted in Figure 1) correspond to copolymers in the literature,[29] PHPT and PPTF, respectively, and the main difference is that the oligomers under study substitute ethylhexyl with methyl at the 9-position in fluorene and at the 10-position in phenothiazine, for the sake of reducing the time of calculation. It has been proven that the presence of alkyl groups does not significantly affect the equilibrium geometry and thus the electronic and the optical properties.[50,51] In fact, many oligomers and polymers were considered as anti conformation in quantum-chemical calculations, so in this study we choose the energetically favorable trans-configuration in the following calculations. The selected important dihedral angles, inter-ring bond lengths, and torsional angles (which are between two adjacent PTZ rings or between the joint PTZ and fluorene rings) in $(PTZ)_n$ and $(FPTZ)_n$ ($n = 1-4$) in the neutral ground state obtained by DFT//B3LYP/6-31G* calculations are listed in Table 1. The results of the optimized structures for the two series of polymeric molecules show that the bond lengths and bond angles do not suffer appreciable variation with the oligomer size in the series of $(PTZ)_n$, as well as $(FPTZ)_n$.[52] It also suggests that we can describe the basic structures of the polymers as their oligomers.

TABLE 1. Selected Dihedral Angles, Inter-ring Bond Distances, and Inter-ring Torsional Angles of $(PTZ)_n$ and $(FPTZ)_n$ ($n = 1-4$) Obtained by DFT//B3LYP/6-31G* Calculations

	dihedral angles (deg)			inter-ring
oligomer	Φ (1,2,3,4)	Φ (3,4,5,6)	inter-ring	distances (Å)
$(PTZ)_n$				
$n = 1$	35.9	40.2		
$n = 2$	36.0	39.5	35.8	1.482
$n = 3$	36.2	38.9	35.5	1.482
$n = 4$	35.9	39.3	35.1	1.482
$(FPTZ)_n$				
$n = 1$	36.1	39.2	36.7	1.483
$n = 2$	36.0	39.3	36.4	1.483
$n = 3$	35.9	38.9	36.5	1.483
$n = 4$	35.8	38.8	36.5	1.483

As already mentioned, one of the most important features of the π-conjugated polymers is their ability to become highly conducting after oxidative (p-type)[53] or reductive (n-type)[54] doping. Thus, the cationic and anionic geometries of oligomers in both series of $(PTZ)_n$ and $(FPTZ)_n$ ($n = 1-4$) are optimized by B3LYP/6-31G*, and bond lengths and dihedral angles corresponding to the ground states are compiled in Table 2. For the sake of investigating the structural variation with the adding or extracting an electron, the contour plots of HOMO and LUMO orbitals of the oligomers $(PTZ)_n$ and $(FPTZ)_n$ ($n = 1-4$) by B3LYP/6-31G* are also plotted in Figure S2 (Supporting Information.)[52] The optimized ionic geometries were then used to calculate the ionization potential and electron affinity energies.

The energy gap has been estimated in two ways, namely, HOMO−LUMO gaps and the lowest excited energies. We employed the linear extrapolation technique in this research,[56] which has been successfully employed to investigate several series of polymers.[57−60] The linearity between the calculated IPs, EAs, Δ_{H-L}'s, and E_g's of the oligomers and the reciprocal

(48) Klaerner, G.; Miller, R. D. *Macromolecules* **1998**, *31*, 2007−2009.

(49) Frisch, M. J.; Trucks, G. W.; Schlegel, H. B.; Scuseria, G. E.; Robb, M. A.; Cheeseman, J. R.; Montgomery, J. A., Jr.; Vreven, T.; Kudin, K. N.; Burant, J. C.; Millam, J. M.; Iyengar, S. S.; Tomasi, J.; Barone, V.; Mennucci, B.; Cossi, M.; Scalmani, G.; Rega, N.; Petersson, G. A.; Nakatsuji, H.; Hada, M.; Ehara, M.; Toyota, K.; Fukuda, R.; Hasegawa, J.; Ishida, M.; Nakajima, T.; Honda, Y.; Kitao, O.; Nakai, H.; Klene, M.; Li, X.; Knox, J. E.; Hratchian, H. P.; Cross, J. B.; Adamo, C.; Jaramillo, J.; Gomperts, R.; Stratmann, R. E.; Yazyev, O.; Austin, A. J.; Cammi, R.; Pomelli, C.; Ochterski, J. W.; Ayala, P. Y.; Morokuma, K.; Voth, G. A.; Salvador, P.; Dannenberg, J. J.; Zakrzewski, V. G.; Dapprich, S.; Daniels, A. D.; Strain, M. C.; Farkas, O.; Malick, D. K.; Rabuck, A. D.; Raghavachari, K.; Foresman, J. B.; Ortiz, J. V.; Cui, Q.; Baboul, A. G.; Clifford, S.; Cioslowski, J.; Stefanov, B. B.; Liu, G.; Liashenko, A.; Piskorz, P.; Komaromi, I.; Martin, R. L.; Fox, D. J.; Keith, T.; Al-Laham, M. A.; Peng, C. Y.; Nanayakkara, A.; Challacombe, M.; Gill, P. M. W.; Johnson, B.; Chen, W.; Wong, M. W.; Gonzalez, C.; Pople, J. A. Gaussian 03, Revision B.04, Gaussian, Inc., Pittsburgh, PA, 2003.

(50) Foresman, J. B.; Head-Gordon, M.; Pople, J. A. *J. Phys. Chem.* **1992**, *96*, 135.

(51) Belletête, M.; Beaypré, S.; Bouchard, J.; Blondin, P.; Leclerc, M.; Durocher, G. *J. Phys. Chem. B* **2000**, *104*, 9118.

(52) The selected optimized bond lengths, bond angles and dihedral angles are included in Table S1. The optimized structures of all the oligomers in both series are plotted in Figure S1. The electron density isocontours of HOMO and LUMO of the oligomers in $(PTZ)_n$ and $(FPTZ)_n$ ($n = 1\sim4$) by B3LYP/6-31G* are plotted in Figure S2.

(53) Agrawal, A. K.; Jenekhe, S. A. *Chem. Mater.* **1996**, *8*, 579.

(54) Ho, P. K. H.; Kim, J.-S.; Burroughes, J. H.; Becker, H.; Lis, S. F. Y. Brown, T. M.; Cacialli, F.; Friend, R. H. *Nature* **2000**, *404*, 481.

(55) Rajendra, R.; Abdelwahed, S. H.; Guzei, I. A. *J. Am. Chem. Soc.* **2003**, *125*, 8712−8713.

(56) Kwon, O.; McKee, M. L. *J. Phys. Chem. A* **2000**, *104*, 7106.

TABLE 2. Selected Dihedral Angles, Inter-ring Bond Distances, and Inter-ring Torsional Angles of $(PTZ)_n$ and $(FPTZ)_n$ ($n = 1-4$) in Cationic and Anionic States Obtained by DFT//B3LYP/6-31G* Calculations

oligomer	dihedral angles (deg) Φ (1,2,3,4)	Φ (3,4,5,6)	inter-ring	inter-ring distances (Å)
$(PTZ)_n$				
	cationic state			
$n = 1$	15.6	20.3		
$n = 2$	26.7	26.2	23.9	1.465
$n = 3$	29.4	27.1	27.8	1.472
$n = 4$	30.4	29.5	28.8	1.475
	anionic state			
$n = 1$	41.8	22.7		
$n = 2$	34.4	33.2	13.2	1.446
$n = 3$	34.8	32.1	21.2	1.462
$n = 4$	33.7	32.5	25.0	1.468
$(FPTZ)_n$				
	cationic state			
$n = 1$	21.6	24.1	25.4	1.464
$n = 2$	28.1	28.4	30.3	1.475
$n = 3$	30.0	30.6	32.1	1.479
$n = 4$	30.9	32.4	34.1	1.480
	anionic state			
$n = 1$	35.1	32.7	15.1	1.451
$n = 2$	33.7	34.3	24.8	1.469
$n = 3$	34.1	35.2	28.3	1.475
$n = 4$	34.0	35.5	30.2	1.478
$n = 1$	35.1	32.7	15.1	1.451

chain length is excellent for both homologous series of oligomers. The nature and the energy of the first 10 singlet−singlet electronic transitions have been obtained by TD-DFT/B3LYP calculations performed on the B3LYP/6-31G*-optimized geometries, respectively, and the results are compared with the available experimental data. The excited geometries were optimized by ab initio CIS/3-21G*.[61] On the basis of the excited geometries, the emission spectra of monomers of the two series are investigated.

3. Results and Discussion

3.1. Optimized Geometry. 3.1.1. Ground-State Geometry. From Table 1, we notice that the PTZ moiety is highly nonplanar (as depicted in Figure 2) and its structure tends to be bending in a butterfly-like shape across the line fixed by the sulfur and nitrogen atoms with the average values of dihedral angles Φ(1,2,3,4) and Φ(3,4,5,6) in the oligomers of PPTZ around 36° and 39°, respectively. This nonplanar geometry is due to the presence of two heteroatoms with different atom radii and suggests minimal molecular orbital overlap between the sulfur or nitrogen and the joint atoms. Moreover, one PTZ ring is twisted by about 35° relative to the adjacent PTZ ring, suggesting some charge delocalization between the two rings. On the contrary, because the dihedral angle between two phenyl rings in the fluorene segment of the series of oligomers of PFPTZ is fixed by ring bridged atoms which tend to keep their normal tetrahedral angles in their ring linkage, the fluorenes keep their quasiplanar conformation, and the dihedral angles in them are no more than 1°. In fact, in the pristine state, polyfluorene emits in the deep blue spectral region. During operation there appears, however, an additional emission peak at around 2.3 eV. This observation has usually been attributed to aggregate or excimer formation due to the planar conformation. Recently, carbazole-based π-conjugated polymers were shown to successfully achieve negligible low-energy emission bands.[61c] In this study, however, PTZ ring is introduced into the PF π-conjugation backbone. One particularly striking difference between the carbazole and phenothiazine rings is that the former is planar whereas the latter is highly nonplanar. In the copolymer PFPTZ, the PTZ ring still maintains the high nonplanarity as it presented in PPTZ. The PTZ rings are twisted by about 36° from the adjacent fluorene plane, which is slightly larger than that between the adjacent PTZ rings in PPTZ. A consequence of the highly nonplanar geometry of the PTZ in the alternating copolymer PFPTZ has been proved to efficiently impede π-stacking aggregation and intermolecular excimer formation, resulting in identical dilute solution and solid-state photophysics.[29,30]

3.1.2. Frontier Molecular Orbitals. It will be useful to examine the highest occupied orbitals and the lowest virtual orbitals for these oligomers and polymers because the relative ordering of the occupied and virtual orbitals provides a reasonable qualitative indication of the subsequent excitation properties[62] and of the ability of electron or hole transport. The electron density isocontours of HOMO and LUMO of the oligomers in $(PTZ)_n$ and $(FPTZ)_n$ ($n = 1-4$) by B3LYP/6-31G* are plotted in Figure S2 (Supporting Information).[52]

Figure S2 (Supporting Information) shows that all frontier obitals in the oligomers of both series under study spread over the whole π-conjugated backbone, although the largest contributions come from the different part of the chromophores. There is antibonding between the bridge atoms of the inter-ring, and there is bonding between the bridge carbon atom and its conjoint atoms of the intra-ring in the HOMO. On the contrary, there is bonding in the bridge single bond of the inter-ring and antibonding between the bridge atom and its neighbor of the intra-ring in the LUMO. In general, the HOMO possesses an antibonding character between the subunits. This may explain the nonplanarity observed for these oligomers in their ground states. On the other hand, the LUMO of all the oligomers generally shows a bonding character between the subunits. This implies that the singlet excited state involving mainly the promotion of an electron from the HOMO to the LUMO should be more planar. It is noteworthy that in the copolymer PFPTZ the electronic cloud distribution is strongly confined to PTZ rings in the HOMO, whereas for LUMO, the electronic clouds transfer to the fluorene rings from the PTZ rings and mainly constrain in fluorene moieties. For polymers, this implies the PTZ serves as electron-donating functionalities by the pres-

(57) Wang, J. F.; Feng, J. K.; Ren, A. M.; Liu, X. D.; Ma, Y. G.; Lu, P.; Zhang, H. X. *Macromolecules* **2004**, *37*, 3451.
(58) Brédas, J. L.; Silbey, R.; Boudreaux, D. S.; Chance, R. R. *J. Am. Chem. Soc.* **1983**, *105*, 6555.
(59) Ma, J.; Li, S. H.; Jiang, Y.-S. *Macromolecules* **2002**, *35*, 1109.
(60) (a) Ford, W. K.; Duke, C. B.; Salaneck, W. R. *J. Chem. Phys.* **1982**, *77*, 5030. (b) Ford, W. K.; Duke, C. B.; Paton, A. *J. Chem. Phys.* **1982**, *77*, 4564.
(61) (a) Yang, L.; Ren, A. M.; Feng, J. K.; Liu, X. D.; Ma, Y. G.; Zhang, H. X. *Inorg. Chem.* **2004**, *43*, 5961. (b) Yang, L.; Ren, A. M.; Feng, J. K.; Ma, Y. G.; Zhang, M.; Liu, X. D.; Shen, J. C.; Zhang, H. X. *J. Phys. Chem.* **2004**, *108*, 6797. (c) Yang, L.; Ren, A. M.; Feng, J. K. *J. Comput. Chem.* **2005**, *26*, 969. (d) Yang, L.; Ren, A. M.; Feng, J. K. *J. Org. Chem.* **2005**, *70*, 3009.
(62) De Oliveira, M. A.; Duarte, H. A.; Pernaut, J. M.; De Almeida, W. B. *J. Phys. Chem. A* **2000**, *104*, 8256.

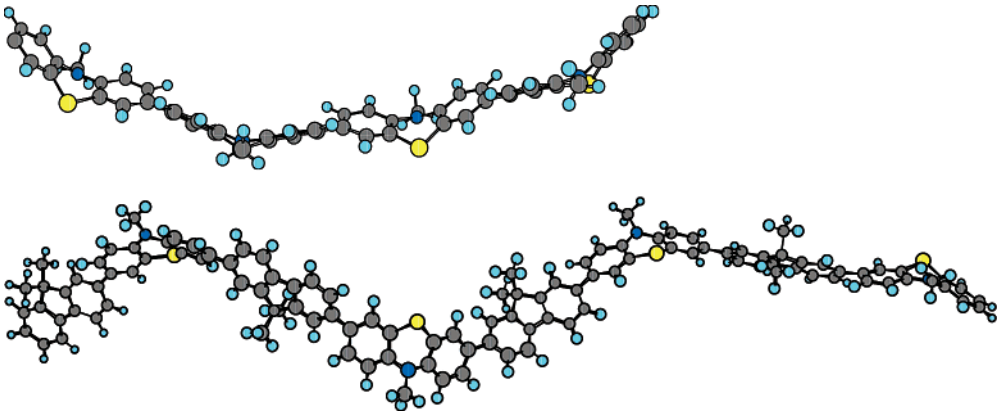

FIGURE 2. Optimized structures of $(PTZ)_4$ (up) and $(FPTZ)_4$ (down).

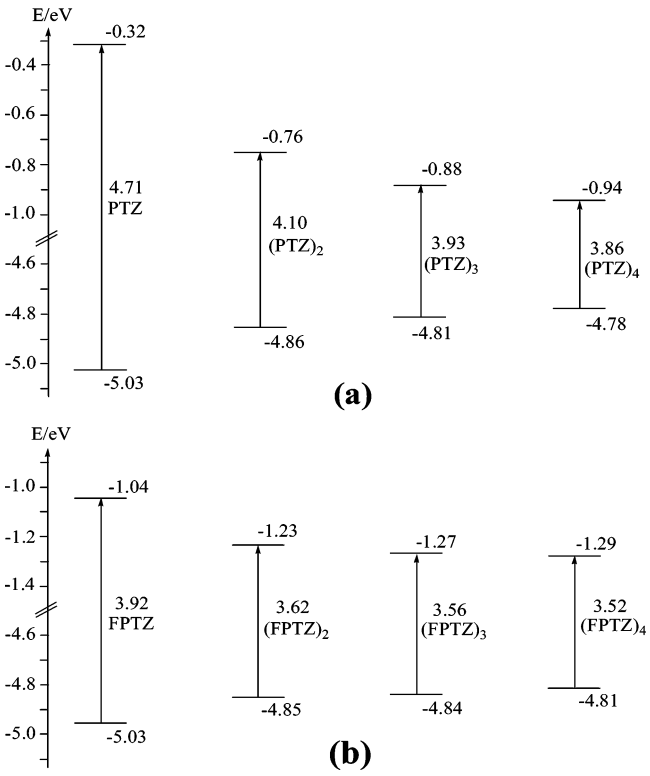

FIGURE 3. Energy levels of HOMO and LUMO of $(PTZ)_n$ (a) and $(FPTZ)_n$ (b) ($n = 1-4$) obtained by B3LYP/6-31G*.

ence of the electron-rich sulfur and nitrogen heteroatoms, and it is anticipated that PFPTZ have reduced ionization potential owing to a strong electron-donating groups on the conjugation backbone.

In the experiments, the HOMO and LUMO energies were calculated from one empirical formula proposed by Brédas et al., based on the onset of the oxidation and reduction peaks measured by cyclic voltammetry, assuming the absolute energy level of ferrocene/ferrocenium to be 4.4 eV below vacuum.[33] Whereas the HOMO and LUMO energies can be calculated accurately by density functional theory (DFT) in this study. The energy levels of HOMO and LUMO of the oligomers in $(PTZ)_n$ and $(FPTZ)_n$ ($n = 1-4$) by B3LYP/6-31G* are plotted in Figure 3a,b.

From parts a and b of Figure 3, it can be seen that with the increasing conjugation lengths the HOMO energies increase, whereas the LUMO energies decrease in both series. The observed 0.25 eV difference between the monomer and quadmer is rather small compared to other monomer/quadmer systems such as thiophene-based (0.44 eV)[63] and fluorene (0.63 eV)[57] systems. The main reason is that electronic delocalization is limited by the nonplanar geometry of the phenothiazine ring. Interestingly, there is only a small shift of the HOMO energy of the quadmer of PFPTZ (HOMO = 4.81 eV), containing alternating phenothiazine and fluorenes, compared to the monomer of PPTZ. This means that there is even less electronic coupling between two phenothiazine rings separated by the fluorene moiety. Most importantly, the HOMO energies in both PPTZ and PFPTZ (~ -4.8 eV) dramatically increase about 0.4 eV than PF (~ -5.2 eV),[57] indicating that the electron-donating PTZ units significantly improve the hole-accepting properties and result in more efficient charge carrier balance. The highly nonplanar property of PTZ is decisive to the high energy level of HOMOs, since the HOMOs are dominated by contribution from the PTZ moieties. As far as the LUMO energies are concerned, they are around ~ -1.2 eV in PF,[57] nearly equal to that in PFPTZ (~ -1.2 eV), suggesting the introduction of PTZ does not worsen the electron-accepting ability of the fluorene-based copolymers.

3.1.3. The Geometry in the Cationic and Anionic States. Compared the results in Tables 1 and 2, we can find the structural variation in cationic and anionic states relative to the neutral ground states. One can see that the inter-ring distances between the two adjacent subunits decrease in the both cationic and anionic states in the oligomers of $(PTZ)_n$, as well as the series of $(FPTZ)_n$. The shortening of the inter-ring distances in ionic states relative to that in neutral state can easily be seen from the HOMO and LUMO characters plotted in Figure S2 (Supporting Informatoion). There is antibonding between the bridge atoms of inter-ring and there is bonding between the bridge carbon atom and its conjoint atoms of intra-ring in the HOMO. Hence, removing an electron from HOMO leads to a shortening of the inter-ring distances in cationic state relative to the neutral state. On the other hand, the LUMO of all the oligomers generally shows a bonding character between the subunits. The shortening of the inter-ring distance in the

(63) Zhou, X.; Ren, A. M.; Feng, J. K. *Polymer* **2004**, *45*, 7705.

TABLE 3. Ionization Potentials, Electron Affinities, and Extraction Potentials for Each Molecule (in eV)[a]

oligomer	IP(v)	IP(a)	HEP	EA(v)	EA(a)	EEP
$(PTZ)_n$						
$n = 1$	6.70	6.49	6.31	1.30	1.11	0.89
$n = 2$	6.05	5.89	5.75	0.44	0.24	0.06
$n = 3$	5.76	5.65	5.55	0.08	0.05	0.19
$n = 4$	5.59	5.51	5.43	0.12	0.22	0.31
$n = \infty$	5.29	5.23	5.17	0.40	0.30	0.10
exptl	5.0[b]					
$(FPTZ)_n$						
$n = 1$	6.26	6.10	5.96	0.20	0.02	0.16
$n = 2$	5.73	5.64	5.55	0.36	0.47	0.58
$n = 3$	5.52	5.45	5.39	0.60	0.68	0.75
$n = 4$	5.38	5.33	5.29	0.73	0.79	0.84
$n = \infty$	5.13	5.13	5.10	0.81	1.00	1.06
exptl	5.1[b]					

[a] The suffixes (v) and (a) indicate vertical and adiabatic values, respectively. [b] Ionization potential was obtained based on IP = E_{ox}^{onset} + 4.4 eV (where E_{ox}^{onset} is onset oxidation potentials vs SCE and the SCE energy level of −4.4 eV below the vacuum level is used).

anionic state is due to the bonding interactions between the π orbitals on the two adjacent moieties. On the other hand, the injection of electrons or holes in these oligomers of both series induces to the better conjugations and the whole molecules tend to more planar than their corresponding neutral ground states. In the cationic state of both series of PPTZ and PFPTZ, the torsional angles, Φ(1,2,3,4) and Φ(3,4,5,6) of PTZ rings are even smaller than that in their anionic state. This is because the HOMO orbitals are mainly localized on PTZ rings, whereas the LUMO orbitals are predominant π bonding character of fluorene rings, the injection of a hole has much effects on HOMO and thus on the structure of PTZ. However, as for the inter-ring dihedral angles, they twist less in the anionic states than that in their cationic states, since the HOMO shows inter-ring antibonding character and LUMO shows inter-ring bonding character. Indeed, the injection of an electron should enhance the bonding character of LUMO and thus enhance the electronic conjugation over the whole molecular structure in the anionic states.

3.2. Ionization Potentials and Electron Affinities. The adequate and balanced transport of both injected electrons and holes are important in optimizing the performance of OLED devices. The ionization potential (IPs) and electron affinity (EAs) are well-defined properties that can be calculated by DFT to estimate the energy barrier for the injection of both holes and electrons into the polymer. Table 3 contains the ionization potentials (IPs), electron affinities (EAs), both vertical (v; at the geometry of the neutral molecule) and adiabatic (a; optimized structure for both the neutral and charged molecule), and extraction potentials (HEP and EEP for the hole and electron, respectively) that refer to the geometry of the ions.[64] The IPs, EAs, HEPs, and EEPs for infinite chains of the polymers were determined by plotting these values of oligomers against the reciprocal of the number of modeling polymeric units and by extrapolating the number of units to infinity. It can be seen from Table 3 that the ionization potentials (IP)or HOMO levels of PHPT and PPTF based on the empirical formula IP = E_{ox}^{onset} + 4.4 eV are estimated to be 5.0 and 5.1 eV, respectively,[29] which agree well with our extrapolated IPs with the values of average 5.2 and 5.1 eV for PPTZ and PFPTZ. The experimental data are slightly larger than the calculated HOMO energy levels of 4.8 eV for both systems.

One general challenge for the application of polyfluorenes in PLEDs is achievement of high electron affinity (n-type) conjugated polymers for improving electron injection/transport and low ionization potential (p-type) conjugated polymers for better hole injection/transport in polymer electronic devices. For PPTZ and PFPTZ, the energies required to create a hole in the polymers are around 5.2 and 5.1 eV, respectively, which are lower than that in PF (5.4 eV).[57] Thus, hole injection and transportation from PPTZ to the copolymer PFPTZ are expected to be easier than to the PF, and as a consequence, the charge carrier balance is better in the devices constructed from the copolymers. Interestingly, from our calculations, it seems that the copolymers have superior properties than the pristine phenothiazine and fluorene polymers. While the extraction of an electron from the anion requires average ∼0.4, 0.3, and 0.1 eV by three methods for PPTZ, respectively, which indicates the worse electron-accepting ability of PPTZ. In the copolymer PFPTZ, however, the EAs are around 1.0 eV, which changes little compared with that in the corresponding PF (∼1.2 eV),[57] suggesting that the electron-accepting properties in the copolymer PFPTZ do not worsen.

TABLE 4. HOMO−LUMO Gaps (Δ_{H-L}) (eV) by B3LYP and the Lowest Excitation Energies (E_g) (eV) by TDDFT of $(PTZ)_n$ and $(FPTZ)_n$ (n = 1−4)

oligomers	Δ_{H-L}	E_g(TD)	oligomers	Δ_{H-L}	E_g(TD)
$(PTZ)_n$			$(FPTZ)_n$		
$n = 1$	4.71	3.90	$n = 1$	3.92	3.48
$n = 2$	4.10	3.58	$n = 2$	3.62	3.23
$n = 3$	3.92	3.41	$n = 3$	3.56	3.18
$n = 4$	3.85	3.37	$n = 4$	3.52	3.15
$n = \infty$	**3.55**	**3.20**	$n = \infty$	**3.38**	**3.03**
expl		2.77	expl		2.81

3.3. HOMO−LUMO Gaps and the Lowest Excitation Energies. There are two theoretical approaches for evaluating the energy gap in this paper. One way is based on the ground-state properties, from which the band gap is estimated from the energy difference between the highest occupied molecular orbital (HOMO) and the lowest unoccupied molecular orbital (LUMO),[65] when $n = \infty$, termed the HOMO−LUMO gaps (Δ_{H-L}'s). The TDDFT, which has been used to study systems of increasing complexity due to its relatively low computational cost and also to include in its formalism the electron correlation effects, is also employed to extrapolate energy gap of polymers from the calculated first dipole-allowed excitation energy of their oligomers.

Here, the HOMO−LUMO gaps (Δ_{H-L}'s) and lowest singlet excited energies (E_g) are both listed in Table 4

(64) (a)Curioni, A.; Boero, M.; Andreoni, W. *Chem.Phys. Lett.* **1998**, *294*, 263−271. (b) Wang, I.; Estelle, B. A.; Olivier, S.; Alain, I.; Baldeck, P. L. *J. Opt. A: Pure Appl. Opt*. **2002**, *4*, S258−S260.

(65) (a) Jeffrey Hay, P. *J. Phys. Chem. A* **2002**, *106*, 1634−1641. (b) Curioni, A.; Andreoni, W.; Treusch, R.; Himpsel, F. J.; Haskal, E.; Seidler, P.; Heske, C.; Kakar, S.; van Buuren, T.; Terminello, L. J. *Appl. Phys. Lett.* **1998**, *72*, 1575−1577. (c) Hong, S. Y.; Kim, D. Y.; Kim, C. Y.; Hoffmann, R. *Macromolecules* **2001**, *34*, 6474−6481.

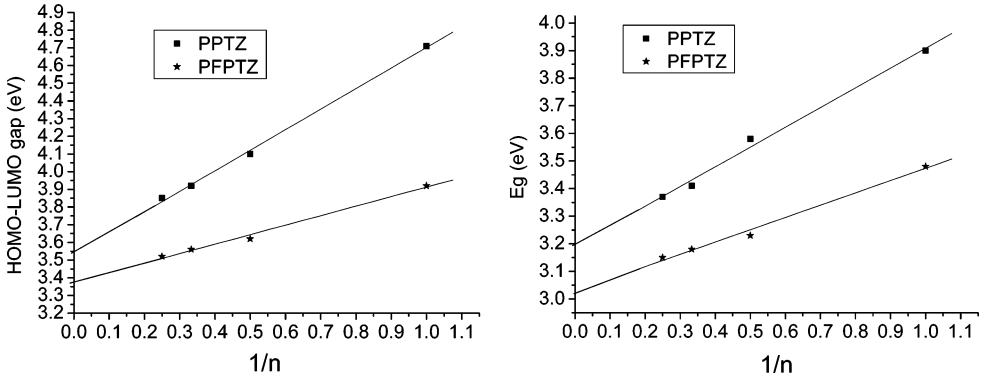

FIGURE 4. HOMO−LUMO gaps by B3LYP and the lowest excitation energies E_g's by TD-DFT as a function of reciprocal chain length n in oligomers of $(PTZ)_n$ and $(FPTZ)_n$.

and the relationships between the calculated Δ_{H-L} and the E_g and the inverse chain length are plotted in Figure 4. There is a good linear relation between the energy gaps by both methods and the inverse chain length. Indeed, as shown in Table 4 the B3LYP/6-31G* HOMO−LUMO energy gaps (Δ_{H-L}) are found to be higher than the TDDFT//B3LYP/6-31G* energies of the corresponding HOMO−LUMO transitions. It is because that the energy of the vertical electronic transition from a doubly occupied MO to a vacant MO is predicted to be smaller than their energy gap, what must be ascribed to the reduced interelectronic interaction upon the single one-electron excitation (i.e., the interaction can be conceptually interpreted in a simple way as the balance between coulomb and exchange terms, and expectedly it should decrease progressively with increasing size of the π-conjugated system).[66]

Obviously, the E_g presented in Table 4 yields a good agreement with the experimental data than Δ_{H-L} in both series in this study.[29] However, there are still errors between the calculated results and the experimental values from the edge of the electronic band; this discrepancy is in part due to the relatively large size of the studied systems and the reciprocal dependence of the energy gap on the number of repeat units usually observed in organic systems. Another factor responsible for deviations by both methods from experimental is that the predicted band gaps are for the isolated gas-phase chains, while the experimental band gaps are measured in the liquid phase where the environmental influence may be involved. Additionally, it should be borne in mind that solid-state effects (like polarization effects and intermolecular packing forces) have been neglected in the calculations. The latter can be expected to result in a decreased inter-ring twist and consequently a reduced gap in a thin film compared to an isolated molecule as considered in the calculations.[67,68] In fact, although the approach to get band gap with orbital energy difference between the HOMO and LUMO is crude considering experimental comparison, it is desirable to obtain the useful information in the nature of the lowest singlet excited state. Because the HOMO−LUMO gap is easy to get, the approach can also be used to provide valuable information on estimate band gaps of oligomers and polymers, especially treating even larger systems.

As one can see the energy gaps obtained by TD-DFT and HOMO−LUMO gaps in PPTZ are both higher than that in PFPTZ with corresponding methods. It seems that this result is reverse to the experimental observations.[30] According to our calculations, since the HOMOs are constrained in the PTZ rings, both series of oligomers have similar HOMO energy levels; however, in PFPTZ the LUMOs are mainly localized on the fluorene rings, which are lower than that in PPTZ and thus resulting in the lower energy gaps than PPTZ. On the other hand, the results obtained with TDDFT show that for the lowest excited states in both series the pair HOMO−LUMO gives the major contribution, nearly 65% of the transition. In fact, the observed band gaps of the copolymers in the ref 30 were found to decrease as the fraction of PTZ in the copolymers increased. Indeed, our calculations actually are in favor of the experimentally observed and at the same time the calculated outcomes predict that when the ratio of fluorene and PTZ is 1:1 or less than 1, the energy gaps in copolymer PFPTZ even decrease below PPTZ.[29] On all accounts, the results of both methods indicate that the incorporation with electron-donating moieties PTZ will reduce the band gaps of fluorene-based copolymers due to the highly nonplanar structure in PTZ, which resulting in the high HOMO energy level, and with the fractions of the PTZ increasing, the band gaps decrease. So we can estimate that the narrower band gaps of both PPTZ and PFPTZ would lead to the red-shifted absorption and emission wavelengths.

3.5. Absorption spectra. The TDDFT//B3LYP/6-31G* has been used on the basis of the optimized geometry to obtain the nature and the energy of 10 singlet−singlet electronic transitions of all the oligomers in both series under study and only the most relevant singlet−singlet excited states with strong oscillator strengths ($f > 0.01$) in PPTZ and PFPTZ are reported in Tables 5 and 6. Three interesting trends can be observed in both series of oligomers: (1) in the considerable broad regions, the electronic states exhibit large f values with no clear peak; (2) the oscillator strengths (f) of the lowest $S_0 \rightarrow S_1$ electronic transition are the largest in both series of oligomers, except for the monomer of PPTZ and PFPTZ,

(66) Brière, J. F.; Côté, M. *J. Phys. Chem. B* **2004**, *108*, 3123.
(67) Puschning, P.; Ambrosch-Draxl, C.; Heimel, G.; Zojer, E.; Resel, R.; Leising, G.; Kriechbaum, M.; Graupner, W. *Synth. Met.* **2001**, *116*, 327.
(68) Eaton, V. J.; Steele, D. *J. Chem. Soc., Faraday Trans. 2* **1973**, *2*, 1601.

TABLE 5. Electronic Transition Data Obtained by the TDDFT//B3LYP/6-31G* for $(PTZ)_n$

electronic transitions	wavelength (nm)	f	MO/character	coefficient
PTZ				
$S_1 \leftarrow S_0$	317.38	0.0000	HOMO → LUMO	0.67
$S_2 \leftarrow S_0$	286.94	0.0216	HOMO → LUMO+1	0.65
$S_3 \leftarrow S_0$	283.37	0.0686	HOMO → LUMO+2	0.61
$S_4 \leftarrow S_0$	243.51	0.0424	HOMO → LUMO+3	0.65
$S_5 \leftarrow S_0$	240.56	0.1111	HOMO → LUMO+4	0.63
$S_6 \leftarrow S_0$	236.30	0.2482	HOMO-1 → LUMO	0.51
			HOMO → LUMO+4	0.34
$S_8 \leftarrow S_0$	222.05	0.0119	HOMO-1 → LUMO	0.60
$(PTZ)_2$				
$S_1 \leftarrow S_0$	346.10	0.2682	HOMO → LUMO	0.64
$S_4 \leftarrow S_0$	303.03	0.2130	HOMO → LUMO+4	0.45
			HOMO → LUMO+1	0.33
$S_5 \leftarrow S_0$	296.31	0.0196	HOMO → LUMO+2	0.62
$S_6 \leftarrow S_0$	293.24	0.0825	HOMO → LUMO+3	0.52
			HOMO-1 → LUMO+2	0.21
$S_7 \leftarrow S_0$	286.30	0.0533	HOMO-1 → LUMO+1	0.60
$S_{10} \leftarrow S_0$	271.95	0.1526	HOMO-1 → LUMO+2	0.58
			HOMO-2 → LUMO	0.20
$(PTZ)_3$				
$S_1 \leftarrow S_0$	363.62	0.5414	HOMO → LUMO	0.65
$S_2 \leftarrow S_0$	339.33	0.0314	HOMO-1 → LUMO	0.54
			HOMO → LUMO+1	0.27
$S_3 \leftarrow S_0$	335.23	0.0395	HOMO-2 → LUMO	0.51
			HOMO-1 → LUMO+1	0.36
$S_6 \leftarrow S_0$	306.46	0.1706	HOMO → LUMO+7	0.38
			HOMO-1 → LUMO+1	0.34
$S_7 \leftarrow S_0$	303.38	0.0153	HOMO → LUMO+3	0.47
			HOMO → LUMO+5	0.30
$S_9 \leftarrow S_0$	301.16	0.0879	HOMO → LUMO+7	0.37
			HOMO-1 → LUMO+1	0.36
$S_{10} \leftarrow S_0$	294.34	0.0413	HOMO → LUMO+4	0.53
			HOMO-1 → LUMO+6	0.28
$(PTZ)_4$				
$S_1 \leftarrow S_0$	367.08	0.8639	HOMO → LUMO	0.64
$S_2 \leftarrow S_0$	349.73	0.0307	HOMO-1 → LUMO	0.50
			HOMO → LUMO+1	0.36
$S_3 \leftarrow S_0$	335.18	0.0689	HOMO-2 → LUMO+1	0.43
			HOMO-1 → LUMO+1	0.32
$S_{10} \leftarrow S_0$	305.52	0.0136	HOMO → LUMO+8	0.27
			HOMO-3 → LUMO	0.24
			HOMO → LUMO+4	0.22
expt	285[a]			

[a] Measured for thin films on fused quartz plates.

TABLE 6. Electronic Transition Data Obtained by the TDDFT//B3LYP/6-31G* for $(FPTZ)_n$

electronic transitions	wavelength (nm)	f	MO/character	coefficient
FPTZ				
$S_1 \leftarrow S_0$	355.60	0.2866	HOMO → LUMO	0.65
$S_2 \leftarrow S_0$	311.82	0.0639	HOMO → LUMO+1	0.65
$S_3 \leftarrow S_0$	296.24	0.2498	HOMO → LUMO+2	0.52
			HOMO-1 → LUMO	0.27
$S_4 \leftarrow S_0$	290.35	0.2417	HOMO → LUMO+3	0.45
			HOMO-1→ LUMO	0.36
$S_5 \leftarrow S_0$	286.93	0.5644	HOMO-1→ LUMO	0.40
			HOMO → LUMO+2	0.38
$S_6 \leftarrow S_0$	281.86	0.1437	HOMO→ LUMO+4	0.55
			HOMO-2→ LUMO	0.20
$S_7 \leftarrow S_0$	262.41	0.0122	HOMO-1→ LUMO+2	0.47
			HOMO-4 → LUMO	0.34
$S_9 \leftarrow S_0$	258.74	0.0157	HOMO-2→ LUMO	0.58
			HOMO → LUMO+4	0.18
$(FPTZ)_2$				
$S_1 \leftarrow S_0$	384.38	1.0447	HOMO → LUMO	0.65
$S_2 \leftarrow S_0$	363.90	0.1098	HOMO-1 → LUMO	0.62
$S_3 \leftarrow S_0$	350.06	0.0643	HOMO → LUMO+1	0.60
			HOMO-1 → LUMO	0.23
$S_4 \leftarrow S_0$	328.70	0.0096	HOMO-1 → LUMO+1	0.63
$S_5 \leftarrow S_0$	317.58	0.0607	HOMO-1 → LUMO+2	0.47
			HOMO → LUMO+3	0.26
$(FPTZ)_3$				
$S_1 \leftarrow S_0$	390.28	1.6401	HOMO → LUMO	0.64
$S_2 \leftarrow S_0$	375.86	0.0136	HOMO-1 → LUMO	0.50
			HOMO → LUMO+1	0.30
$S_3 \leftarrow S_0$	363.26	0.2522	HOMO-2 → LUMO	0.43
			HOMO → LUMO+1	0.34
$S_5 \leftarrow S_0$	348.82	0.1192	HOMO → LUMO+2	0.36
			HOMO-1 → LUMO+2	0.30
$S_6 \leftarrow S_0$	344.16	0.0579	HOMO-1 → LUMO+1	0.45
			HOMO → LUMO+2	0.36
$S_{10} \leftarrow S_0$	318.73	0.0241	HOMO → LUMO+3	0.49
			HOMO → LUMO+8	0.17
			HOMO-2 → LUMO+8	0.16
$(FPTZ)_4$				
$S_1 \leftarrow S_0$	393.67	2.0835	HOMO → LUMO	0.63
$S_2 \leftarrow S_0$	379.60	0.1082	HOMO-1 → LUMO	0.46
			HOMO → LUMO+1	0.42
$S_3 \leftarrow S_0$	364.79	0.1981	HOMO-2 → LUMO	0.41
			HOMO-1 → LUMO+1	0.31
$S_4 \leftarrow S_0$	358.41	0.1132	HOMO → LUMO+1	0.33
			HOMO-1 → LUMO+2	0.28
			HOMO-3 → LUMO	0.27
$S_7 \leftarrow S_0$	345.24	0.0921	HOMO → LUMO+1	0.37
			HOMO-2 → LUMO+1	0.32
$S_9 \leftarrow S_0$	327.11	0.0283	HOMO → LUMO+1	0.37
			HOMO-2 → LUMO+1	0.32
expt	373			

[a] Measured for thin films on fused quartz plates.

in which although $S_0 \rightarrow S_2$ and $S_0 \rightarrow S_1$ feature relative high f values, $S_0 \rightarrow S_6$ and $S_0 \rightarrow S_5$ electronic transitions exhibit the largest ones, respectively; (3) the oscillator strength coupling the lowest CT $\pi-\pi^*$ singlet excited state to the ground state increase strongly when going from an isolated molecule to a molecular group and this trend goes along with the conjugation lengths increasing.

All electronic transitions are of the $\pi\pi^*$ type, and no localized electronic transitions are exhibited among the calculated singlet−singlet transitions. Excitation to the S_1 state corresponds almost exclusively to the promotion of an electron from the HOMO to the LUMO. As in the case of the oscillator strength, the absorption wavelengths arising from $S_0 \rightarrow S_1$ electronic transition increase progressively with the conjugation lengths increasing. It is reasonable, since HOMO → LUMO transition is predominant in $S_0 \rightarrow S_1$ electronic transition and as analysis above that with the extending molecular size, the HOMO−LUMO gaps decrease.

As shown in Table 5, each oligomer of PPTZ has a rather broad absorption with no clear peak in nearly 70 nm regions. Taking $(PTZ)_4$ as an example whose character is relative close to the polymer, it has a strong absorption in the 367−305 nm range with absorption maxima at around 367 and 335 nm, respectively. In the case of the phenothiazine-fluorene alterating copolymer, $(FPTZ)_4$, it exhibits maximum UV−vis absorption at around 410 and 380 nm, respectively, within the broad absorption band ranging from 410 to 337 nm. The related polyfluorene homopolymer has an intense structureless absorption center at 370 nm. These results show that the ground-state electronic structure of the alternating copolymer PFPTZ is completely different from those of the related homopolymers by the presence of the highly nonplanar PTZ moiety. It can be seen that the UV−vis absorption spectrum of PFPTZ exhibited red-shifted from

that of the PPTZ, in agreement with the energy gaps determined from the absorption onset.

From Tables 5 and 6 we find the TDDFT results systematically overestimated the observed absorption spectra in experiment and this goes along with the increase conjugation lengths. Many investigations show that TDDFT is a good predictive tool for absorption spectra of molecules. However, this method has defects to study extended systems. Because it is not infrequent that the optical properties reach saturation already for quite short chain length, whereas the orbital energies still continue to change for longer oligomers. It is known that the exchange-correlation (XC) functionals must decrease with increasing chain length (this trend of variation is in line with the expectation that in more extended systems the electronic repulsion is smaller).[69,70] However, reasonable results can still be expected here, because (1) we use the HF/DFT hybrid functionals B3LYP, which could partially overcome the asymptotic problem,[71] and because (2) we study the homologous fluorene-based cooligomers and polymers, with our interests in their relative excitation energies to those pristine polyfluorene. The results show that slightly longer maximal absorption wavelength in the series of PFPTZ are observed than that of PPTZ due to different PTZ fractions. Compared with PF (∼368 nm by TDDFT),[57] the absorption spectra exhibit bathochromic shift in PFPTZ by the introduction of electron-donating group PTZ. All these conclusions basically consist with experimental observed.[29,30]

3.6. Properties of Excited Structures and Emission Spectra. Density functional methods in the Gaussian program package are, however, incapable of geometry optimization in designated excited states because of a lack of efficient algorithms for analytical gradients. Until now, the standard for calculating excited state equilibrium properties of larger molecules is the configuration interaction singles (CIS) method. However, due to the neglect of electron correlation, CIS results are not accurate enough in many applications. In this study, we hope to investigate the excited state properties by this method, in despite of not accurate. Because the calculation of excited-state properties typically requires significantly more computational effort than is needed for the ground states and dramatically constrains by the size of the molecules, we only optimize the monomer and dimer of PPTZ and monomer of PFPTZ by CIS/3-21G*. In Figure 5 we take FPTZ as an example to compare the excited structures of PFPTZ by CIS/3-21G* with their ground structures by HF/3-21G*. Interestingly, the main characters of the front orbitals by HF/3-21G* are the same to that by B3LYP/6-31G*. As shown, some of the bond lengths lengthened, but some shortened. We can predict the differences of the bond lengths between the ground (S_0) and singlet excited state (S_1) from MO nodal patterns. Since the singlet state corresponds to an excitation from the HOMO to the LUMO in all considered oligomers, we can explore the bond lengths variation by

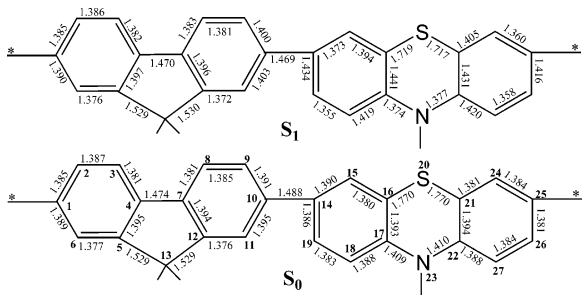

FIGURE 5. Comparison of the excited structure (S_1) by CIS/3-21G* with the ground geometry (S_0) by HF/3-21G* of FPTZ.

analyzing the HOMO and LUMO. The HOMO is bonding across *r*(14,19), *r*(16,17), *r*(17,18), *r*(21,22), and *r*(22,27) bonds in FPTZ, but the LUMO has nodes in these regions. Therefore, one would expect elongation of these bonds; the data in the figure shows that these bonds are in fact considerably longer in the excited state. The HOMO has a node across the r(5,6), *r*(4,7), *r*(8,9), *r*(11,12), and *r*(10,14) bonds in FPTZ, while the LUMO is bonding. The data confirm the anticipated contraction of these bonds.

The dihedral angles Φ(16,20,21,22) and Φ(17,23,-22,21) in PTZ, $(PTZ)_2$, and FPTZ reduced from 37° and 38° by HF/3-21G* to nearly 29° and 13° by CIS/3-21G*, respectively. The bridge bonds between each conjugation segment rotate to some extent when excited from ground to excited states. The inter-ring torsional angles in $(PTZ)_2$ and FPTZ decrease from 49° and 50° to 36° and 34°, respectively. It is obvious that the excited structure has a strong coplanar tendency in both of the series; that is, the conjugation is better in the excited structure, which further approves the predictions from frontier orbitals.

Consequently, the emission calculations are made by reoptimizations of the PTZ, $(PTZ)_2$, and FPTZ with the CIS/3-21G* method in their first singlet excited states, followed by using the resulting geometries to perform TD calculations employing the B3LYP/3-21G* method from the singlet ground state to the first five singlet excited states, and the results are tabulated in Table 7. The calculated emission spectra of PTZ, $(PTZ)_2$, and FPTZ shown in Table 7 reveal that they are nearly identical; the slight difference is that $(PTZ)_2$ has a peak at 347 nm whereas that of FPTZ is at 353 nm. Although there are some discrepancies between the calculated values and the observed data,[29,30] they have the same trend that the emission peaks exhibit slight bathochromic shift in FPTZ compared with $(PTZ)_2$, due to different PTZ fractions. Furthermore, the fluorescent peaks with strongest intensity in PTZ, $(PTZ)_2$ and FPTZ all arise from $S_2 \rightarrow S_0$ $\pi\pi^*$ electron transition dominated by HOMO → LUMO+2 (62%), HOMO-1 → LUMO (61%) and HOMO → LUMO+1 (65%), respectively. Most importantly, even though a slightly red-shifted occurs in the PTZ-containing polymers compared with PF, greenish-blue electronluminescence was successfully achieved.[29,30]

In addition, comparing Tables 5 and 6 with Table 7, the rather large Stokes shift of around 0.7 eV observed in these oligomers must thus be explained by an alternative mechanism. We note that the phenothiazine ring is highly nonplanar in the ground state, impeding sufficiently π-stacking aggregation and intermolecular ex-

(69) Grimme, S.; Parac, M. *ChemPhysChem* **2003**, *3*, 292.
(70) Ortiz, R. P.; Delgado, M. C. R.; Casado, J.; Hernandez, V.; Kim, O. K.; Woo, H. Y.; Lopez Navarrete, L. *J. Am. Chem. Soc.* **2004**, *126*, 13363.
(71) Gao, Y.; Liu, C.; Jiang, Y. *J. Phys. Chem. A* **2002**, *106*, 5380.
(2) Hsu, C.; Hirata, S.; Martin, H. *J. Phys. Chem. A* **2001**, *105*, 451.

TABLE 7. Electronic Transition Data Obtained by the TDDFT//B3LYP/3-21G* Based on the CIS/3-21G* Geometries for the Monomer and Dimer of PPTZ and Monomer of PFPTZ

electronic transitions	wavelength (nm)	*f*	MO/character	coefficient	wavelength expt/nm
PTZ					
$S_1 \rightarrow S_0$	406.44	0.0021	HOMO → LUMO	0.67	
$S_2 \rightarrow S_0$	307.04	0.0873	HOMO → LUMO+2	0.62	
$S_3 \rightarrow S_0$	298.89	0.0324	HOMO → LUMO+1	0.63	
$S_4 \rightarrow S_0$	246.74	0.0005	HOMO → LUMO+4	0.69	
$S_5 \rightarrow S_0$	245.90	0.0438	HOMO → LUMO+3	0.60	
			HOMO-2 → LUMO	0.30	
$(PTZ)_2$					
$S_1 \rightarrow S_0$	438.08	0.0944	HOMO → LUMO	0.65	478[a]
$S_2 \rightarrow S_0$	347.09	0.2225	HOMO-1 → LUMO	0.61	476[b]
$S_3 \rightarrow S_0$	339.26	0.1100	HOMO → LUMO+1	0.60	
$S_4 \rightarrow S_0$	317.31	0.1169	HOMO → LUMO+3	0.46	
			HOMO → LUMO+2	0.44	
$S_5 \rightarrow S_0$	309.77	0.0153	HOMO → LUMO+4	0.63	
FPTZ					
$S_1 \rightarrow S_0$	437.68	0.1457	HOMO → LUMO	0.64	478[a]
$S_2 \rightarrow S_0$	353.99	0.1837	HOMO → LUMO+1	0.65	480[b]
$S_3 \rightarrow S_0$	312.61	0.0058	HOMO → LUMO+2	0.56	
			HOMO → LUMO+4	0.26	
$S_4 \rightarrow S_0$	306.08	0.0156	HOMO → LUMO+3	0.55	
			HOMO → LUMO+2	0.30	
$S_5 \rightarrow S_0$	298.37	0.0677	HOMO → LUMO+4	0.51	
			HOMO → LUMO+3	0.28	

[a] PL spectra maxima of the polymer films. [b] EL spectra maxima of the EL devices.

cimer formation. On the other hand, we observe that the phenothiazine ring and even the whole molecular structures of PPTZ and PFPTZ in the excited state are more planar than that in the ground state. Consequently, the relaxed singlet excited state from which emission occurs is lower lying than if photoinduced planarization were absent.

4. Conclusion

The presence of the electron-rich sulfur and nitrogen heteroatoms results in the highly nonplanar conformations in phenothiazine ring relative to the rigid planar structures in fluorene ring. The highly nonplanar structural properties in the homopolymer PPTZ and alternating copolymer PFPTZ impede π-stacking aggregation and intermolecular excimer formation, resulting in identical dilute solution and solid-state photophysics, which hampers the application of polyfluorenes in PLEDs. All decisive molecular orbitals are delocalized on all subunits of the oligomers. The HOMO possesses an antibonding character between subunits, which may explain the nonplanarity observed for these oligomers in their ground state. On the other hand, the LUMO shows bonding character between the two adjacent rings, in agreement with the more planar S_1 excited state. Importantly, electron-donating groups PTZ not only enhance the optical stability and thus increase fluorescence quantum yields, but also improve the hole injection and more efficient charge carrier balance due to the higher HOMO levels and the lower IPs, compared with those of conventional polyfluorene materials. These two points are essential for light-emitting polymers and provide the opportunity to tune the electronic and optical properties of the resulting polymers.

Our calculated results also indicate that the incorporation with electron-donating moieties PTZ will reduce the band gaps of fluorene-based copolymers due to the highly nonplanar structure in PTZ, which resulting in the high HOMO energy level, and with the fractions of the PTZ increasing, the band gaps decrease. Both PPTZ and PFPTZ have rather broad absorption bands and have two absorption maximum, which is completely different from those of the related fluorene polymers. The absorption and emission spectra of $(FPTZ)_n$ exhibit red-shifted compared with $(PTZ)_n$ ascribed to the different PTZ fractions and the two series both emit a greenish-blue light.

Finally, this theoretical study confirmed experimental results where it was shown that by modification of chemical structures could greatly modulate and improve the electronic and optical properties of pristine polymers. Furthermore, using theoretical methodologies, we showed that is possible to predict reasonably the electronic properties of conjugated systems and we are convinced that the systematic use of those theoretical tools should contribute to orientate the synthesis efforts and help understand the structure-properties relation of these conjugated materials.

Acknowledgment. This work is supported by the Major State Basis Research Development Program (No. 2002CB 613406), the National Nature Science Foundation of China (No. 90101026), and the Key Laboratory for Supramolecular Structure and Material of Jillin University.

Supporting Information Available: Optimized structures and coordinates of the structures. This material is available free of charge via the Internet at http://pubs.acs.org.

JO050665P